Thermal Properties and Solvent Polarities of Mixed-Valence Ionic Liquids Containing Cationic Biferrocenylene Derivatives

Hamada, Shota

Mochida, Tomoyuki

Thermal Properties and Solvent Polarities of Mixed-Valence Ionic Liquids Containing Cationic Biferrocenylene Derivatives

Shota Hamada[†] and Tomoyuki Mochida*[†‡]

[†]*Department of Chemistry, Graduate School of Science, Kobe University, 1-1 Rokkodai, Nada, Kobe, Hyogo 657-8501, Japan. E-mail: tmochida@platinum.kobe-u.ac.jp*

[‡]*Research Center for Membrane and Film Technology, Kobe University, 1-1 Rokkodai, Nada, Kobe, Hyogo 657-8501, Japan*

ABSTRACT: Ionic liquids (ILs) containing cationic mixed-valence biferrocenylene derivatives were synthesized with an octanoyl or octyl substituent in each cation. Their melting points ranged between 25 and 39 °C and the octanoyl derivatives exhibited higher melting points than the octyl derivatives. In addition, each IL exhibited a glass transition in the temperature ranging from −66 to −45 °C after melting. Their melting points were ~10 °C higher than those of mononuclear octamethylferrocenium salts bearing the same substituents. The solvent polarity (E_T^N) and Kamlet-Taft parameters (π^*, α, and β) of these dinuclear and mononuclear ILs were then examined. The dinuclear ILs bearing octanoyl substituents exhibited significant increases in E_T^N and π^*, and a decrease in α with decreasing temperature, whereas the other ILs exhibited a significantly less pronounced temperature dependence. Finally, the intervalence charge-transfer (or charge-resonance) bands of the octanoyl dinuclear ILs exhibited red-shifts with decreasing temperature, which can be regarded as self-thermosolvatochromism.

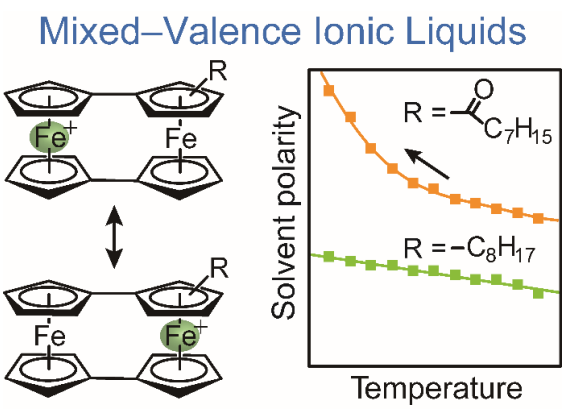

INTRODUCTION

In recent decades, extensive investigations have been conducted into the science and application of ionic liquids (ILs).[1] Although the majority of ILs are composed of salts based on onium cations, a number of metal-containing ILs have also been reported,[2–10] which exhibit unique functions originating from the constituent metal complexes. In addition, our laboratory has developed a variety of organometallic ILs containing mononuclear sandwich complexes, such as ferrocenium cations.[11–19] These organometallic ILs exhibit intriguing magnetic properties,[13,14] photoreactivities,[15–18] and chemical reactivities.[19]

In this study, we aimed to prepare ILs based on cationic dinuclear organometallic complexes. Multinuclear complexes are interesting because of their mixed-valency properties, although room temperature ILs based on multinuclear complexes are scarce.[20–22] The monocations of biferrocene (**Figure 1a**)[23–33] and 1,1-biferrocenylene (**Figure 1b**, bis(fulvalene)diiron; BFD)[27,28,34–41] are typical examples of mixed-valence compounds. According to the Robin-Day classification, mixed-valence compounds can be classified as Class I (non-interacting), Class II (moderately coupled), and Class III (strongly coupled) compounds depending on the coupling between the two redox centers.[28,42–45] Mixed-valence complexes exhibit intervalence charge-transfer bands,[42–45] although the term intervalence charge resonance (IVCR) is more appropriate for the bands in Class III compounds because charge transfer is not responsible for the absorption.[34,46] The biferrocenium monocation, containing one Fe(II) and one Fe(III) center, typically exhibits Class II behavior.[23–33] This cation undergoes rapid valence tautomerization coupled with intramolecular electron transfer, in addition to often exhibiting charge localization at low temperatures. In contrast, BFD is a Class III average-valence complex,[28,34–41] even when unsymmetrically substituted.[34,38] In this complex, the interaction between the two metal centers is strong enough to give a genuinely averaged valence state, where the valence tautomers of BFD form the resonance structures (**Figure 1b**). We were interested in whether such dinuclear organometallic cations can produce ILs. In addition, ILs with

mixed-valence cations may exhibit intriguing solvent properties owing to their large polarizability. Previously, we synthesized salts of biferrocenium cations and bis(trifluoromethanesulfonylamide) (Tf_2N) anions, although they were found to be solids with high melting points.[26] We therefore considered preparing the salts of BFD cations in this study.

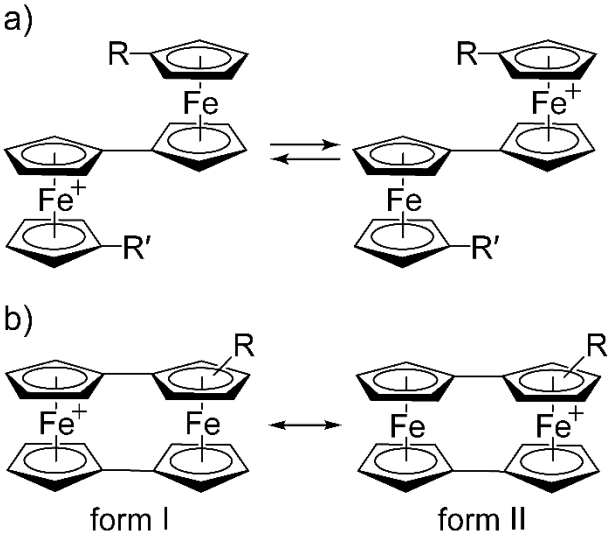

Figure 1. Structures of the monocations of (a) biferrocene (tautomeric structures) and (b) BFD (resonance structures).

Thus, we herein report the thermal properties and solvent polarities of mixed-valence ILs containing cationic dinuclear BFD derivatives and the Tf_2N anion (**Figure 2a**). Cations containing an octyl or octanoyl substituent at the α- or β-position are employed, and the properties of the obtained ILs (**1a, 1b, 2a,** and **2b**) are discussed in comparison with those of mononuclear ferrocenium ILs **3** and **4** (**Figure 2b**), whose molecular volumes are similar to those of the dinuclear ILs. Compound **3** is synthesized for the first time in this study, whereas the preparation and thermal properties of **4** have been previously reported.[14] In addition, we evaluate the solvent polarity parameters (E_T^N and the Kamlet-Taft parameters)[47–49] of the synthesized ILs, noting that the solvent polarity parameters of a number of onium-based ILs have been previously measured using solvatochromic dyes,[49–60] including their temperature dependence.[61–65] Finally, the solvato- and thermochromic properties of

the IVCR bands of the dinuclear ILs are examined.

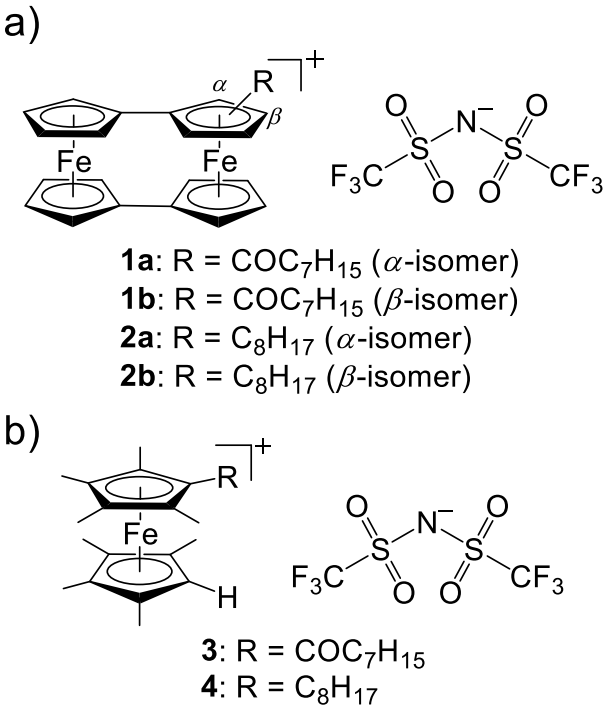

Figure 2. Structural formulae of (a) dinuclear ILs **1a**/**1b** and **2a**/**2b**, and (b) mononuclear ILs **3** and **4**.

RESULTS AND DISCUSSION

Thermal properties. Dinuclear ILs **1a**–**2b** were obtained as dark green crystals by the reaction of neutral BFD derivatives and $AgTf_2N$. The green crystals of mononuclear IL **3** were prepared using the same procedure. The thermal properties of these salts were then investigated by differential scanning calorimetry (DSC), and the results are summarized in **Table 1**, together with those of **4**.[14]

The melting points of the dinuclear ILs were near room temperature (25–39 °C), and they maintained the liquid state at ambient temperature after melting. More specifically, the melting points of acyl derivatives **1a** and **1b** were 37.6 and 38.9 °C, respectively, which were ~10 °C higher than those of alkyl derivatives **2a** and **2b** (i.e., 25.4 and 28.6 °C, respectively). This tendency was ascribed to the higher polarity of the acyl substituents present in the cation component. In each derivative, the β-isomer (**1b** or **2b**) exhibited a slightly higher melting point than that of the α-isomer (**1a** or **2a**), which could be due to the longer molecular shape of the former. Indeed, a similar

tendency has been observed in several BFD derivatives.[35]

We further compared the melting points of the dinuclear ILs and their precursors (neutral BFD derivatives), as shown in **Figure 3**. The neutral BFD derivatives exhibited the same tendency as the salts, with higher melting points being observed for the acyl derivatives and the *β*-isomers. In addition, the melting points of **1a**/**1b** and **2a**/**2b** were 10–20 °C lower than those of their precursors, and a linear correlation was found to exist (i.e., $T_{m(salt,\ °C)} = 0.61 \times T_{m(precursor,\ °C)} + 3.5$). A similar linear correlation was also observed for ferrocenium ILs and their precursors ($T_{m(salt,\ °C)} = 0.94 \times T_{m(precursor,\ °C)} + 30.3$).[11] These correlations suggest that the intermolecular interactions commonly present in the salts and precursors dominate the melting points in both of these organometallic ILs. In contrast to mononuclear ILs, dinuclear ILs generally exhibit lower melting points than their precursors, which may be primarily ascribed to their larger cation volumes.

After melting, the dinuclear ILs maintained their liquid states below room temperature, exhibiting glass transitions at low temperatures. The glass-transition temperatures of **1a**/**1b** and **2a**/**2b** were approximately –45 and –65 °C, respectively, and the ratio of the glass transition temperature to the melting point (T_g/T_m) ranged from 0.69 to 0.73, which is in accordance with the empirical relationship of $T_g/T_m = 2/3$.[66,67] At high temperatures, the acyl derivatives decomposed easily because of the presence of electron-withdrawing substituents. Their decomposition temperatures (**1a**, 70 °C; **1b**, 71 °C) were significantly lower than those of the alkyl derivatives (**2a**, 132 °C; **2b**, 123 °C). As a result, the liquid temperature range ($T_g - T_{dec}$) of the acyl derivatives (i.e., 116 °C) was narrower than that of the alkyl derivatives (i.e., ~190 °C).

Mononuclear ILs **3** and **4** were chosen for comparison because their cation volumes were comparable to those of the dinuclear ILs (V = 316 Å^3 for $[Fe(C_5Me_4H)_2]^+$ and V = 344 Å^3 for $[BFD]^+$, as estimated by DFT calculations). It was found that the acyl derivative **3** (T_m = 28.3 °C) exhibited a higher melting point than the alkyl derivative **4** (T_m = 16.9 °C), which was similar to the case of the dinuclear ILs. In addition, **3** crystallized upon cooling from the melt and exhibited no glass transition.

The melting points of the dinuclear ILs were ~10 °C higher than those of the corresponding mononuclear ILs, which may be due to their higher molecular weights and slightly larger volumes.

Table 1. Thermodynamic data for the dinuclear ILs (**1a/1b** and **2a/2b**), the mononuclear ILs (**3** and **4**), and their corresponding precursors (neutral BFD/ferrocene derivatives)

	Tf_2N salt					Precursor	
	T_m (°C)	ΔS_m (J mol^{-1} K^{-1})	T_g (°C)	T_g/T_m	T_{dec} (°C)	T_m (°C)	ΔS_m (J mol^{-1} K^{-1})
1a	37.6	47.3	−46	0.73	70	56.1	53.2
1b	38.9	49.5	−45	0.73	71	58.3	51.3
2a	25.4	37.5	−66	0.69	132	36.4	42.1
2b	28.6	34.2	−63	0.70	123	41.5	47.5
3	28.3	17.8	–	–		27.2	32.1
4[a)]	16.9	12.5	−84	0.65		23.8	34.7

a) Ref. 14.

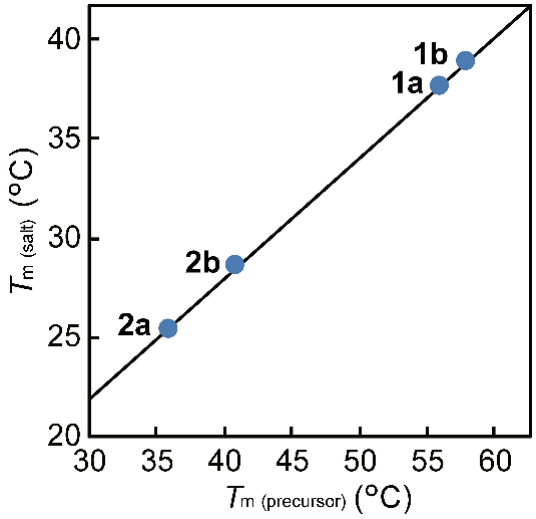

Figure 3. Correlation between the melting points of **1a/1b, 2a/2b,** and their corresponding precursors (neutral biferrocenylenes).

Solvent polarity parameters. The E_T^N and Kamlet-Taft parameters (π^*, α, and β) of the dinuclear and mononuclear ILs in the liquid state were evaluated at 20 °C using solvatochromic dyes, as summarized in **Table 2**. The E_T^N values of these ILs were comparable to those of typical imidazolium-based ILs, although there were some variations depending on the substituents and

cation species employed.

E_T^N is the most widely used empirical scale of solvent polarity, where the values of tetramethylsilane and water are 0 and 1, respectively.[48] The values for the present ILs were determined to be 0.67–0.76, which are comparable to those of alcohols and imidazolium-based ILs containing fluorinated anions (0.5–0.7).[51] More specifically, the E_T^N values for **1a** (0.73) and **1b** (0.76) were larger than those for **2a** (0.70) and **2b** (0.71); the higher values observed for the acyl derivatives are consistent with the substituent polarity, while the larger values observed for the *β*-isomers may be ascribed to their longer cation lengths. Furthermore, the values for these dinuclear ILs were larger than those for mononuclear ILs **3** (0.70) and **4** (0.67), which is consistent with the larger polarizability of the dinuclear units. The acyl derivative also exhibited a larger value for the mononuclear ILs. It should also be noted that the E_T^N values for the current ILs were larger than those of other organometallic ILs containing smaller cations, such as $[Co(C_5H_4Et)_2]Tf_2N$ (0.54)[9] and $[Ru(C_6H_6)(PhBu)]Tf_2N$ (0.51)[12].

The Kamlet-Taft parameters include π^* (dipolarity/polarizability), α (hydrogen-bond donation ability), and β (hydrogen-bond acceptor ability).[49] It was found that the π^* values for **1a**/**1b** and mononuclear ILs **3** and **4** were comparable (i.e., 0.73–0.87). These values are smaller than those generally obtained for imidazolium-based ILs (i.e., ~1),[51–53] and this may be due to their large cation volumes.[68] The reason for the larger values for **2a**/**2b** (i.e., ~1.0) is unclear but it could be due to higher charge delocalization in the cation.

It is known that the value of α (i.e., the hydrogen-bond donation ability) mainly depends on the cation present in the IL.[51] In our case, the values for the current ILs (0.69–0.98) were significantly larger than those of common imidazolium-based ILs (0.4–0.6),[51–53] wherein the larger values obtained for **1a**/**1b** compared to **2a**/**2b** were probably due to the acidity of the ring hydrogen atoms adjacent to the acyl substituents. Consistently, this trend was not observed in the mononuclear ILs (0.8–0.9) containing no ring hydrogen atoms on the substituted ring. In addition, it is known that the

value of β mainly depends on the anion,[51] and hence it is reasonable that the β values of the current ILs (0.21–0.28) are comparable to those of imidazolium-based ILs containing Tf_2N.[51–53]

Table 2. Solvent polarity parameters for **1a/1b, 2a/2b, 3,** and **4** determined at 20 °C and their corresponding temperature dependence

	E_T^N	π^*	α	β	ΔE_T^N a)	$\Delta\pi^*$ a)	$\Delta\alpha$ a)	$\Delta\beta$ a)
1a	0.73	0.77	0.98	0.22	+0.05	+0.28	−0.17	+0.07
1b	0.76	0.85	0.97	0.21	+0.09	+0.44	−0.25	+0.02
2a	0.70	1.03	0.70	0.27	+0.03	+0.16	−0.08	+0.09
2b	0.71	1.05	0.69	0.28	+0.02	+0.08	−0.07	+0.06
3	0.70	0.87	0.83	0.24	+0.02	+0.08	−0.06	+0.05
4	0.67	0.73	0.90	0.24	+0.02	+0.04	−0.03	−0.01
[Bmim]Tf_2N b)	0.64	0.98	0.61	0.24				

a) Difference of the values obtained at 60 and −40 °C. b) Ref. 51.

Temperature dependence of the solvent polarity parameters. The temperature dependence of the solvent polarity parameters of the ILs was then examined between –40 and 60 °C (**Table 2**), within which range all examined ILs maintained their liquid state after melting. As can be seen from **Table 2**, the values of E_T^N, π^*, and α for the dinuclear ILs bearing acyl substituents changed significantly, which is probably ascribed to their unsymmetrical mixed-valence state.

The temperature dependence of the E_T^N values of the ILs is presented in **Fig. 4a**, wherein it can be seen that **1a** and **1b** exhibited significantly higher values at lower temperatures, and the increases in this temperature range (i.e., ΔE_T^N) were +0.05 and +0.09, respectively. The other ILs (i.e., **2a**/**2b, 3,** and **4**) exhibited only a slight, linear increase ($\Delta E_T^N \approx 0.02$); this negative solvatochromic behavior is typically observed in onium-based ILs, and is ascribed to stronger intermolecular interactions at low temperatures.[54,61,63] Notably, the changes observed for **1a**/**1b** were significantly more prominent.

The temperature dependences of the π^* and α values are plotted in **Figures 4b** and **4c**, respectively, wherein it can be seen that the π^* values for acyl derivatives **1a**/**1b** increased markedly

with decreasing temperature. This contrasts with the behavior of the other ILs, which exhibited only a small, linear increase, as typically observed in onium-based ILs, and is consistent with an increase in the liquid density.[63,68] Similarly, the α values of **1a**/**1b** decreased significantly with decreasing temperature, although the other ILs exhibited only a small temperature dependence. The temperature dependence of the β values was small for all ILs ($\Delta\beta$ <0.1; **Figure S2**, Supporting Information).

The observed changes in the solvent polarity parameters for **1a/1b** can likely be attributed to the change in their cation valence state. Of the two resonance structures shown in **Figure 1b**, form I has a greater contribution in the ground state owing to the electron-withdrawing acyl substituent, whereas the contribution of the vibrationally excited state increases at higher temperatures, ultimately leading to a more significant contribution from form II. Therefore, the higher contribution of form I at lower temperatures results in greater charge localization, facilitating ion-pair formation and an increase in the cation dipolarity, which accounts for the increase in the E_T^N and π* values of **1a/1b**. The larger polarity changes in **1b** compared to **1a** may be due to its longer cation length. This interpretation also accounts for the decrease in α at lower temperatures, since the higher contribution from form I leads to the lower acidity of the hydrogen atoms in the substituted ring. Another possibility may be that the effect of ion pairing at low temperatures is more significant in ILs with more polarized cations.

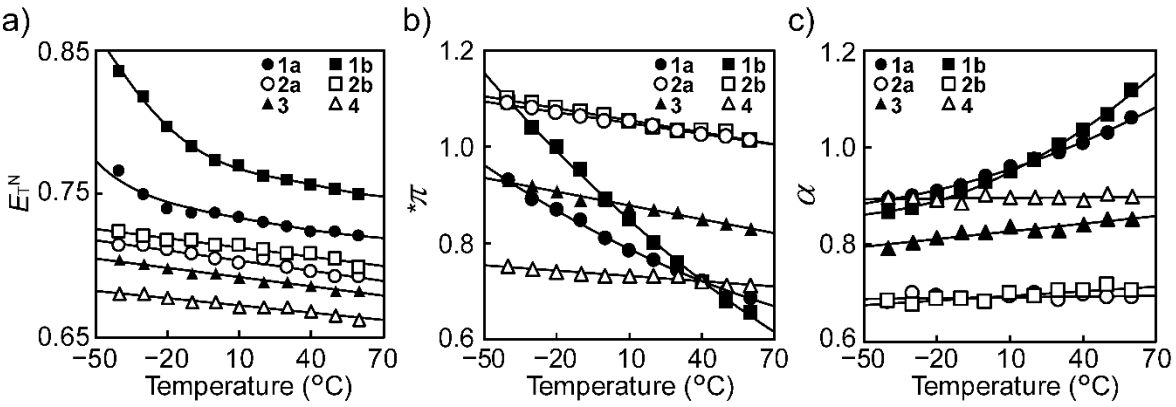

Figure 4. Temperature dependence of the solvent polarity parameters (a) E_T^N, (b) π*, and (c) α for dinuclear ILs **1a/1b** and **2a/2b**, and mononuclear ILs **3** and **4**.

Solvatochromism of the IVCR bands of the dinuclear ILs. The BFD monocation exhibits a particularly broad IVCR band at 1000–2000 nm (5000–10000 cm^{-1}) in solution, which shows only a slight or negligible solvatochromic shift.[34,37,41] We therefore investigated the IVCR energies of the synthesized dinuclear ILs in organic solvents (see **Table 3**), wherein small solvatochromic shifts were observed, albeit smaller than those observed in similar SbF_6 salts.

The IVCR energies of **1a/1b** and **2a/2b** in several organic solvents are plotted in **Figure 5a** as a function of $(1/n^2–1/D)$,[42,45] where n and D are the refractive index and the dielectric constant of the solvent, respectively. As can be seen from the figure, the IVCR energies of **1a**/**1b** exhibited solvatochromic shifts of ~100 cm^{-1} (~7860 cm^{-1} in $CHCl_3$ and ~7960 cm^{-1} in MeCN), whereas the those of **2a**/**2b** exhibited much smaller shifts of ~20 cm^{-1} (~7780 cm^{-1} in $CHCl_3$ and ~7800 cm^{-1} in MeCN). The solvatochromic shifts of the present salts are significantly smaller than those reported for the $SbCl_6$ salts of acetyl and ethyl derivatives.[34] This phenomenon is ascribed to the effect of the Tf_2N anion, which is more coordinating than SbF_6; the polar anion stabilizes the cation through ion pairing or coordination effects,[69] which results in larger IVCR energies, particularly in nonpolar solvents. The larger shifts in the acyl derivatives compared to the alkyl derivatives were attributed to the unsymmetrical cation charge distribution, wherein the charge-resonance transition acquires some charge-transfer character. The solvatochromic shifts of BFD cations are significantly smaller than those of Class II mixed-valence biferrocenium cations (~1000 cm^{-1}, $B(C_6F_5)_4$ salt).[69]

Table 3. Absorption maxima of the IVCR bands for **1a/1b** and **2a/2b** measured in various organic solvents

	$CHCl_3$ (0.270)[a]	THF (0.375)[a]	C_2H_5OH (0.497)[a]	CH_3CN (0.527)[a]	CH_3OH (0.535)[a]
1a	7865	7920	7965	7960	7955
1b	7845	7895	7955	7965	7970
2a	7770	7775	7780	7785	7790
2b	7795	7800	7815	7815	7820

a) Value of $1/n^2–1/D$ of the solvent.

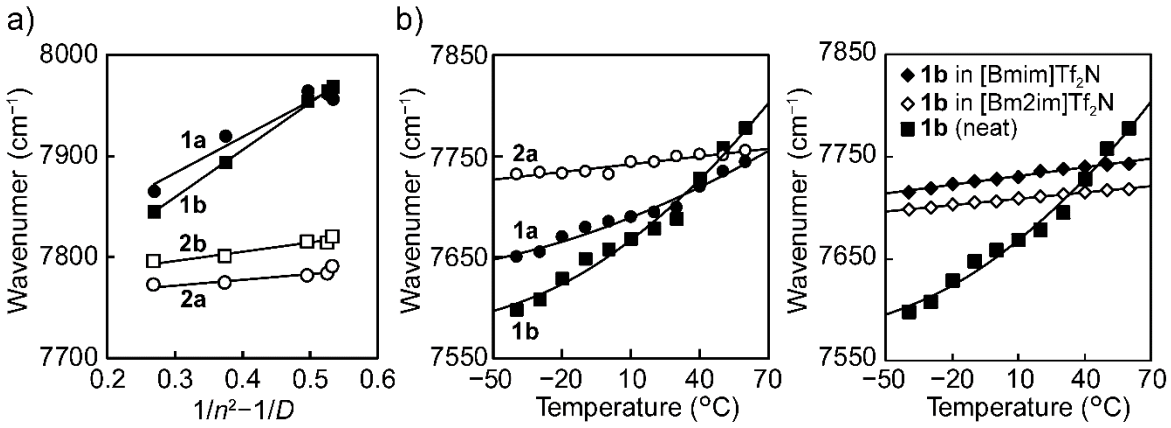

Figure 5. (a) IVCR energies of the dinuclear ILs in organic solvents plotted as a function of ($1/n^2$-$1/D$), where n and D are the refractive index and the dielectric constant of the solvent, respectively. (b) Temperature dependence of the absorption maxima (ν_{max}) of the IVCR bands of **1a**, **1b**, and **2a** in the liquid state, and those of (c) neat **1b**, **1b** in [Bmim]Tf_2N, and **1b** in [Bm2im]Tf_2N.

Thermochromism of the IVCR bands. The IVCR energies of acyl derivatives **1a**/**1b** in the liquid state were examined and compared with those of alkyl derivative **2a**. It was found that the IVCR bands of the neat acyl derivatives exhibited red shifts with respect to those measured in organic solvents, which was ascribed to the effect of the IL environment. Furthermore, the IVCR bands exhibited significant red shifts with decreasing temperature, which is regarded as self-thermosolvatochromism.

The IVCR bands of **1a** and **1b** were observed at 7695 and 7680 cm^{-1}, respectively. The UV-vis-NIR spectrum of **1b** is shown in **Figure S3** (Supporting Information), wherein the observed IVCR bands appeared at lower energies (~200 cm^{-1}) than those measured in $CHCl_3$. To investigate the origin of this effect, we measured the IVCR bands of **1b** dissolved in the [Bmim]Tf_2N (Bmim = 1-butyl-3-methyl-imidazolium) and [Bm2im]Tf_2N (Bm2im = 1-butyl-2,3-dimethylimidazolium) ILs. These bands appeared at 7735 and 7710 cm^{-1}, respectively, which are close to the band of **1b** in the neat state. Therefore, the red shifts can be attributed to the solvent effect in the IL environment. On the other hand, the IVCR band of **2a** appeared at 7745 cm^{-1}, and was shifted by only 25 cm^{-1} with

respect to that in $CHCl_3$. This small shift is consistent with the negligible effect of the solvent on the IVCR energy of **2a**, as described above.

Furthermore, we investigated the temperature dependence of the IVCR energy, as shown in **Figure 5b**. The IVCR energies of **1a** and **1b** exhibited significant red shifts with decreasing temperature, and the shift was more prominent for **1b**. In contrast, **2a** exhibited only a small linear shift. The IVCR energies of **1b** dissolved in [Bmim][Tf_2N] and [Bm2im]Tf_2N were also investigated (**Figure 5c**), where only small temperature dependences were observed. These results indicate that the large thermochromic shifts observed in **1a/1b** in the liquid state is ascribed to their temperature-dependent solvent property changes, rather than their IL environment. Therefore, this phenomenon can be regarded as self-thermosolvatochromism. In addition, the temperature dependence of the IVCR energies in **1a/1b** shows an inflection point at the glass transition temperature, below which these compounds exhibit only a small temperature dependence (**Figure S4**, Supporting Information). This can be accounted for by considering that solvent reorganization does not occur in the glassy state; hence, this result supports the above interpretation. However, the mechanisms behind the red shifts of the IVCR energies of **1a/1b** compared to those observed in organic solvents and at low temperatures remain unclear. The obtained results seem to indicate that the ground state of the cation is destabilized when more strongly solvated in the IL state, which seems contrary to expectation.

CONCLUSION

Organometallic ILs containing mixed-valence biferrocenylenium cations bearing octanoyl or octyl substituents were synthesized, and their thermal properties and solvent polarity parameters were compared with those of mononuclear ILs containing substituted octamethylferrocenium cations. Despite their heavier molecular weights, the melting points of the dinuclear ILs were also detected at approximately room temperature, and the liquid state was maintained after melting. The dinuclear

ILs bearing acyl substituents were found to exhibit a large temperature dependence on the solvent polarity parameters. Furthermore, the intervalence charge-resonance bands of the acyl derivatives exhibited thermosolvatochromic shifts. This study therefore demonstrated that unique liquid features can be achieved by incorporating polynuclear mixed-valence complexes into ILs.

EXPERIMENTAL SECTION

General. 2,6-Diphenyl-4-(2,4,6-triphenylpyridinium-1-yl) phenolate, *N*-diethylnitroaniline (DENA), and nitroaniline (NA) were purchased from Sigma-Aldrich, Oakwood Chemicals, and Wako Chemicals, respectively. Silver bis(trifluoromethanesulfonyl)amide ($AgTf_2N$)[70] and $[Fe(C_5Me_4H)(C_5Me_4COC_7H_{15})]$[14] were synthesized according to the literature. The octanoyl- and octyl-1,1-biferrocenylenes were prepared using the same method as previously described for the corresponding acetyl and ethyl derivatives, respectively, with the exception that octanoyl chloride was used as a reagent.[35] The yields of the α-octanoyl, β-octanoyl, α-octyl, and β-octyl derivatives after recrystallization from dichloromethane were 35, 36, 41, and 20%, respectively. ^{1}H NMR spectroscopy was carried out using a JEOL JNM-ECL-400 spectrometer. Elemental analyses were performed using a Yanaco CHN MT5 instrument, while DSC measurements were carried out using a TA Instruments Q100 calorimeter at a rate of 10 K min^{-1}. The decomposition temperatures were determined by using an Electrothermal 1201D melting point apparatus, and the accuracy was checked by comparing the data for **1b** with that of its thermogravimetric analysis data. The variable-temperature UV-Vis-NIR absorption spectra were recorded on a JASCO V-570 UV/VIS/NIR spectrometer equipped with a Linkam LTS350 hot stage. The UV-Vis spectra for the solvent polarity measurements were recorded using a mixture of the desired IL (10–20 mg) containing a polarity indicator (0.05 eq.), which was melted and sandwiched between two quartz plates. The solvent polarity parameters E_T^N, π^*, α, and β were calculated from the charge-transfer absorption energies of Reichard's dye, DENA, and NA in the ILs using the following equations: E_T^N

= [(28591/λ_{max})−30.7]/32.4, π^* = (27.52−ν_{DENA})/3.128, α = [(28591/$\nu_{Reichardt}$) −14.6(π^*−0.23) −30.1]/16.5, and β = [(1.035ν_{DENA}−ν_{NA})+2.64]/2.[50–52] The IVCR bands measured in the organic solvents were recorded using a sample content of 0.2 wt%, while those recorded in the ILs were carried out at a sample content of 0.1 mol%.

Preparation of 1a/1b and **2a/2b.** A solution of $AgTf_2N$ (85 mg, 0.22 mmol) in CH_2Cl_2 (8 mL) was added in a dropwise manner to a solution of 2-octanoyl-1,1′-biferrocenylene (100 mg, 0.20 mmol) in CH_2Cl_2 (5 mL). After filtration, the filtrate was placed in a test tube under a nitrogen atmosphere. After allowing the solution to stand for 1 week at 12 °C, green crystals of **1a** were obtained in a 16% yield. Anal. Calcd (%) for $C_{30}H_{30}F_6Fe_2NO_5S_2$ (774.37): C, 46.35; H, 3.90; N, 1.81. Found: C, 46.50; H, 3.95; N, 1.91. The other salts were synthesized using the same procedure. **1b**: Yield 5.2%. Anal. Calcd (%) for $C_{30}H_{30}F_6Fe_2NO_5S_2$ (774.37): C, 46.53; H, 3.90; N, 1.81. Found: C, 46.81; H, 3.42; N, 1.54. **2a**: 12% yield. Anal. Calcd (%) for $C_{30}H_{32}F_6Fe_2NO_4S_2$ (760.04): C, 47.39; H, 4.24; N, 1.84. Found: C, 47.52; H, 4.31; N, 1.91. **2b**: 17% yield. Anal. Calcd (%) for $C_{30}H_{32}F_6Fe_2NO_4S_2$ (760.04): C, 47.39; H, 4.24; N, 1.84. Found: C, 47.52; H, 4.49; N, 1.85.

Preparation of 3. An solution of $AgTf_2N$ (56 mg, 0.15 mmol) in CH_2Cl_2 (5 mL) was added dropwise to a solution of [Fe(C_5Me_4H)($C_5Me_4COC_7H_{15}$)] (50 mg, 0.13 mmol) in CH_2Cl_2 (5 mL). After stirring the solution for 30 min at room temperature, the silver deposits were removed by filtration, and the filtrate was evaporated and extracted with CH_2Cl_2. After drying the combined organic extracts over anhydrous $MgSO_4$, the solvent was filtered, and the filtrate was evaporated under reduced pressure. The desired product was obtained as green crystals in 81% yield (74 mg) by recrystallization of the obtained residue from dichloromethane–diethyl ether. Anal. Calcd (%) for $C_{28}H_{40}F_6FeNO_5S_2$ (704.59): C, 47.73; H, 5.72; N, 1.99. Found: C, 47.55; H, 5.99; N, 1.85.

ASSOCIATED CONTENT

Supporting information

DSC; UV-vis-NIR spectrum; solvent polarity parameters; IVCR energies (PDF)

AUTHOR INFORMATION

Corresponding Author

Tomoyuki Mochida − Department of Chemistry, Graduate School of Science and Research Center for Membrane and Film Technology, Kobe University, Kobe, Hyogo 657-8501, Japan; orcid.org/0000-0002-3446-2145; Phone: +81-78-803-5679; Email: tmochida@platinum.kobe-u.ac.jp

Authors

Shota Hamada − Department of Chemistry, Graduate School of Science, Kobe University, Kobe, Hyogo 657-8501, Japan

Notes

The authors declare no competing financial interest.

ACKNOWLEDGMENTS

This work was financially supported by the KANENHI (no. 20H02756) from the Japan Society for the Promotion of Science (JSPS). We thank R. Sumitani for his help with manuscript preparation.

REFERENCES

(1) Kar, M.; Matuszek, K.; MacFarlane, D. R. Ionic Liquids. In *Kirk–Othmer Encyclopedia of Chemical Technology*; John Wiley & Sons, Inc., 2019, DOI: 10.1002/0471238961.ionisedd.a01.pub2.

(2) Schaltin, S.; Brooks, N. R.; Stappers, L.; Van Hecke, K.; Van Meervelt, L.; Binnemans, K.; Fransaer, J. High Current Density Electrodeposition from Silver Complex Ionic Liquids. *Phys. Chem. Chem. Phys.* **2012**, *14*, 1706–1715.

(3) Branco, A.; Branco, L. C.; Pina, F. Electrochromic and Magnetic Ionic Liquids. *Chem. Commun.* **2011**, *47*, 2300–2302.

(4) Brown, R. J. C.; Dyson, P. J.; Ellis, D. J.; Welton, T. 1-Butyl-3-Methylimidazolium Cobalt Tetracarbonyl [Bmim][$Co(CO)_4$]: A Catalytically Active Organometallic Ionic Liquid. *Chem. Commun.* **2001**, 1862–1863.

(5) Zhang, P.; Gong, Y.; Lv, Y.; Guo, Y.; Wang, Y.; Wang, C.; Li, H. Ionic Liquids with Metal Chelate Anions. *Chem. Commun.* **2012**, *48*, 2334–2336.

(6) Iida, M.; Baba, C.; Inoue, M.; Yoshida, H.; Taguchi, E.; Furusho, H. Ionic Liquids of Bis(alkylethylenediamine)silver(I) Salts and the Formation of Silver(0) Nanoparticles from the Ionic Liquid System. *Chem. Eur. J.* **2008**, *14*, 5047–5056.

(7) Yoshida, Y.; Saito, G. Progress in paramagnetic ionic liquids. In *Ionic Liquids: theory, properties, new approaches*; Kokorin, A., Ed.; InTech, 2011; pp 723–738.

(8) Klingele, J. Low-Melting Complexes with Cationic Side Chains – Phosphonium-, Ammonium- and Imidazolium-Tagged Coordination Compounds. *Coord. Chem. Rev.* **2015**, *292*, 15–29.

(9) Ogawa, T.; Yoshida, M.; Ohara, H.; Kobayashi, A.; Kato, M. A Dual-Emissive Ionic Liquid Based on an Anionic Platinum(II) Complex. *Chem. Commun.* **2015**, *51*, 13377–13380.

(10) Monteiro, B.; Outis, M.; Cruz, H.; Leal, J. P.; Laia, C. A. T.; Pereira, C. C. L. A Thermochromic Europium(III) Room Temperature Ionic Liquid with Thermally Activated Anion-Cation Interactions. *Chem. Commun.* **2017**, *53*, 850–853.

(11) Inagaki, T.; Mochida, T.; Takahashi, M.; Kanadani, C.; Saito, T.; Kuwahara, D. Ionic Liquids of Cationic Sandwich Complexes. *Chem. Eur. J.* **2012**, *18*, 6795–6804.

(12) Komurasaki, A.; Funasako, Y.; Mochida, T. Colorless Organometallic Ionic Liquids from Cationic Ruthenium Sandwich Complexes: Thermal Properties, Liquid Properties, and Crystal Structures of [$Ru(\eta^5\text{-}C_5H_5)(\eta^6\text{-}C_6H_5R)$][X] (X = $N(SO_2CF_3)_2$, $N(SO_2F)_2$, PF_6). *Dalton Trans.* **2015**, *44*, 7595–7605.

(13) Funasako, Y.; Mochida, T.; Inagaki, T.; Sakurai, T.; Ohta, H.; Furukawa, K.; Nakamura, T.

Magnetic Memory Based on Magnetic Alignment of a Paramagnetic Ionic Liquid Near Room Temperature. *Chem. Commun.* **2011**, *47*, 4475–4477.

(14) Funasako, Y.; Inagaki, T.; Mochida, T.; Sakurai, T.; Ohta, H.; Furukawa, K.; Nakamura, T. Organometallic Ionic Liquids from Alkyloctamethylferrocenium Cations: Thermal Properties, Crystal Structures, and Magnetic Properties. *Dalton Trans.* **2013**, *42*, 8317–8327.

(15) Mochida, T.; Maekawa, S.; Sumitani, R. Photoinduced and Thermal Linkage Isomerizations of an Organometallic Ionic Liquid Containing a Half-Sandwich Ruthenium Thiocyanate Complex. *Inorg. Chem.* **2021**, *60*, 12386–12391.

(16) Sumitani, R.; Yoshikawa, H.; Mochida, T. Reversible Control of Ionic Conductivity and Viscoelasticity of Organometallic Ionic Liquids by Application of Light and Heat. *Chem. Commun.* **2020**, *56*, 6189–6192.

(17) Ueda, T.; Tominaga, T.; Mochida, T.; Takahashi, K.; Kimura, S. Photogeneration of Microporous Amorphous Coordination Polymers from Organometallic Ionic Liquids. *Chem. Eur. J.* **2018**, *24*, 9490–9493.

(18) Prodius, D.; Macaev, F.; Stingaci, E.; Pogrebnoi, V.; Mereacre, V.; Novitchi, G.; Kostakis, G. E.; Anson, C. E.; Powell, A. K. Catalytic "Triangles": Binding of Iron in Task-specific Ionic Liquids. *Chem. Commun.* **2013**, *49*, 1915–1917.

(19) Boudalis, A. K.; Rogez, G.; Heinrich, B.; Raptis, R. G.; Turek, P. Towards Ionic Liquids with Tailored Magnetic Properties: $Bmim^{+}$ Salts of Ferro- and Antiferromagnetic Cu^{II}_{3} Triangles. *Dalton Trans.* **2017**, *46*, 12263–12273.

(20) Prodius, D.; Smetana, V.; Steinberg, S.; Wilk-Kozubek, M.; Mudryk, Y.; Pecharsky, V. K.; Mudring, A.-V. Breaking the Paradigm: Record Quindecim Charged Magnetic Ionic Liquids. *Mater. Horiz.* **2017**, *4*, 217–221.

(21) Funasako, Y.; Mori, S.; Mochida, T. Reversible Transformation between Ionic Liquids and Coordination Polymers by Application of Light and Heat. *Chem. Commun.* **2016**, *52*, 6277–6279.

(22) Inagaki, T.; Mochida, T. Reactive Half-Metallocenium Ionic Liquids That Undergo Solventless Ligand Exchange. *Chem. Eur. J.* **2012**, *18*, 8070–8075.

(23) Mochida, T.; Funasako, Y.; Kimata, H.; Tominaga, T.; Sakurai, T.; Ohta, H. Valence Control of Ionic Molecular Crystals: Effect of Substituents on the Structures and Valence States of Biferrocenium Salts with Fluoro Tetracyanoquinodimethanides. *Cryst. Growth Des.* **2017**, *17*, 6020–6029.

(24) Mochida, T.; Funasako, Y.; Akasaka, T.; Uruichi, M.; Mori, H. Valence Engineering of Ionic

Molecular Crystals: Monovalent–Divalent Phase Diagram for Biferrocene–Tetracyanoquinodimethane Salts. *CrystEngComm* **2017**, *19*, 1449–1453.

(25) Mochida, T.; Funasako, Y.; Takazawa, K.; Takahashi, M.; Matsushita, M. M.; Sugawara, T. Chemical Control of the Monovalent-Divalent Electron-Transfer Phase Transition in Biferrocenium-TCNQ Salts. *Chem. Commun.* **2014**, *50*, 5473–5475.

(26) Kimata, H.; Inagaki, T.; Mochida, T. Anion-Ordering Phase Transitions in Biferrocenium and Ferrocenium Salts with the Bis(trifluoromethanesulfonyl)amide Anion. *ACS Omega* **2021**, *6*, 21139–21146.

(27) Barlow, S.; O'Hare, D. Metal−Metal Interactions in Linked Metallocenes. *Chem. Rev.* **1997**, *97*, 637–669.

(28) Morrison, W. H.; Hendrickson, D. N. Electron Transfer in Oxidized Biferrocene, Biferrocenylene, and [1.1]Ferrocenophane Systems. *Inorg. Chem.* **1975**, *14*, 2331–2346.

(29) Hendrickson, D. N. Electron Transfer in Mixed-Valence Complexes in the Solid State. In *Mixed Valency Systems: Applications in Chemistry, Physics and Biology*; Nato Science Series; Prassides, C. K., Ed.; Kluwer: Dordrecht, 1991; Vol. 343, pp 67– 90.

(30) Dong, T. Y.; Hendrickson, D. N.; Iwai, K.; Cohn, M. J.; Geib, S. J.; Rheingold, A. L.; Sano, H.; Motoyama, I.; Nakashima, S. Mixed-Valence Dialkylbiferrocenium Salts: An Explanation for the Observed Temperature Dependence of Electron-Transfer Rates. *J. Am. Chem. Soc.* **1985**, *107*, 7996–8008.

(31) Iijima, S.; Saida, R.; Motoyama, I.; Sano, H. The Temperature Dependence of the Trapped and Averaged-Valence State in Mono-Oxidized Dialkylbiferrocenes. *Bull. Chem. Soc. Jpn.* **1981**, *54*, 1375–1379.

(32) Oda, T.; Nakashima, S.; Okuda, T. Mixed-Valence State of Optically Active 1′,1‴-Bis(2-phenylbutyl)-1,1″-biferrocenium Pentaiodide: Effects of Cation Symmetry and Intermolecular Interaction on Trapped-/Detrapped-Valence States. *Inorg. Chem.* **2003**, *42*, 5376–5383.

(33) Sano, H. Mixed-Valence States of Iron in Binuclear Ferrocene Compounds. *Hyperfine Interact.* **1990**, *53*, 97–112.

(34) Breuer, R.; Schmittel, M. Unsymmetrically Substituted 1,1′-Biferrocenylenes Maintain Class III Mixed-Valence Character. *Organometallics* **2013**, *32*, 5980–5987.

(35) Breuer, R.; Schmittel, M. 1,1′-Biferrocenylenes–The More Redox Stable Ferrocenes! New Derivatives, Corrected NMR Assignments, Redox Behavior, and Spectroelectrochemistry. *Organometallics* **2012**, *31*, 1870–1878.

(36) Warratz, R.; Tuczek, F. Low-Energy Bands of Ferrocene-Ferrocenium Dimers: Bandshape Analysis with a Four-Level Two-Mode Vibronic Coupling Configuration Interaction (VCCI) Model Including Asymmetry. *Inorg. Chem.* **2009**, *48*, 3591–3607.

(37) Warratz, R.; Aboulfadl, H.; Bally, T.; Tuczek, F. Electronic Structure and Absorption Spectra of Biferrocenyl and Bisfulvalenide Diiron Radical Cations: Detection and Assignment of New Low-Energy Transitions. *Chem. Eur. J.* **2009**, *15*, 1604–1617.

(38) Moore, M. F.; Hendrickson, D. N. Electronic Structure of the Triiodide Salt of the Asymmetric, Mixed-Valence Cation (3-Acetylfulvalene)(fulvalene)diiron(1+). *Inorg. Chem.* **1985**, *24*, 1236–1238.

(39) Cowan, D. O.; Levanda, C. Organic Solid State. X. 1,1′-Biferrocenylene[Fe(II)Fe(III)]Salts. *J. Am. Chem. Soc.* **1972**, *94*, 9271–9272.

(40) Mueller-Westerhoff, U. T.; Eilbracht, P. Bisfulvalenediiron and Its Iron(II-III) Mixed Valence System. *J. Am. Chem. Soc.* **1972**, *94*, 9272‑9274.

(41) McManis, G. E.; Nielson, R. M.; Weaver, M. J. Intervalence Electron Transfer in Bicobaltocene Cations: Comparison with Biferrocenes. *Inorg. Chem.* **1988**, *27*, 1827–1829.

(42) Meyer, T. J. Optical and Thermal Electron Transfer in Metal Complexes. *Acc. Chem. Res.* **1978**, *11*, 94–100.

(43) Demadis, K. D.; Hartshorn, C. M.; Meyer, T. J. The Localized-to-Delocalized Transition in Mixed-Valence Chemistry. *Chem. Rev.* **2001**, *101*, 2655–2685.

(44) D'Alessandro, D. M.; Keene, F. R. Current Trends and Future Challenges in the Experimental, Theoretical and Computational Analysis of Intervalence Charge Transfer (IVCT) Transitions. *Chem. Soc. Rev.* **2006**, *35*, 424–440.

(45) Jones, S. C.; Barlow, S.; O'Hare, D. Electronic Coupling in Mixed-Valence Dinuclear Ferrocenes and Cobaltocenes with Saturated Bridging Groups. *Chem. Eur. J.* **2005**, *11*, 4473–4481.

(46) Badger, B.; Brocklehurst, B. Absorption Spectra of Dimer Cations. Part 1.–Olefins. *Trans. Faraday Soc.* **1969**, *65*, 2576–2581.

(47) Reichardt, C.; Welton, T. *Solvents and Solvent Effects in Organic Chemistry,* 4th ed., John Wiley & Sons: New Jersey, 2011.

(48) Reichardt, C. Solvatochromic Dyes as Solvent Polarity Indicators. *Chem. Rev.* **1994**, *94*, 2319–2358.

(49) Kamlet, M. J.; Abboud, J. L. M.; Taft, R. W. An Examination of Linear Solvation Energy Relationships. In *Progress in Physical Organic Chemistry*; John Wiley & Sons, Inc.: Hoboken,

2007; pp 485–630.

(50) Reichardt, C. Polarity of Ionic Liquids Determined Empirically by Means of Solvatochromic Pyridinium *N*-Phenolate Betaine Dyes. *Green Chem.* **2005**, *7*, 339–351.

(51) Crowhurst, L.; Mawdsley, P. R.; Perez-Arlandis, J. M.; Salter, P. A.; Welton, T. Solvent–Solute Interactions in Ionic Liquids. *Phys. Chem. Chem. Phys.* **2003**, *5*, 2790–2794.

(52) Ab Rani, M. A.; Brant, A.; Crowhurst, L.; Dolan, A.; Lui, M.; Hassan, N. H.; Hallett, J. P.; Hunt, P. A.; Niedermeyer, H.; Perez-Arlandis, J. M.; Schrems, M.; Welton, T.; Wilding, R. Understanding the Polarity of Ionic Liquids. *Phys. Chem. Chem. Phys.* **2011**, *13*, 16831–16840.

(53) Chiappe, C.; Pomelli, C. S.; Rajamani, S. Influence of Structural Variations in Cationic and Anionic Moieties on the Polarity of Ionic Liquids. *J. Phys. Chem. B* **2011**, *115*, 9653–9661.

(54) Machado, V. G.; Stock, R. I.; Reichardt, C. Pyridinium *N*-Phenolate Betaine Dyes. *Chem. Rev.* **2014**, *114*, 10429–10475.

(55) Weiß, N.; Schmidt, C. H.; Thielemann, G.; Heid, E.; Schröder, C.; Spange, S. The Physical Significance of the Kamlet-Taft π^* Parameter of Ionic Liquids. *Phys. Chem. Chem. Phys.* **2021**, *23*, 1616–1626.

(56) Wang, X.; Zhang, S.; Yao, J.; Li, H. The Polarity of Ionic Liquids: Relationship between Relative Permittivity and Spectroscopic Parameters of Probe. *Ind. Eng. Chem. Res.* **2019**, *58*, 7352–7361.

(57) Schade, A.; Behme, N.; Spange, S. Dipolarity versus Polarizability and Acidity versus Basicity of Ionic Liquids as a Function of Their Molecular Structures. *Chem. Eur. J.* **2014**, *20*, 2232–2243.

(58) Spange, S.; Lienert, C.; Friebe, N.; Schreiter, K. Complementary Interpretation of $E_T(30)$ Polarity Parameters of Ionic Liquids. *Phys. Chem. Chem. Phys.* **2020**, *22*, 9954–9966.

(59) Thielemann, G.; Spange, S. Polarity of Tetraalkylammonium-based Ionic Liquids and Related Low Temperature Molten Salts. *New J. Chem.* **2017**, *41*, 8561–8567.

(60) Eyckens, D. J.; Henderson, L. C. A Review of Solvate Ionic Liquids: Physical Parameters and Synthetic Applications. *Front. Chem.* **2019**, *7*, 263.

(61) Martins, C. T.; Sato, B. M.; Seoud, O. A. E. First Study on the Thermo-Solvatochromism in Aqueous 1-(1-Butyl)-3-methylimidazolium Tetrafluoroborate: A Comparison between the Solvation by an Ionic Liquid and by Aqueous Alcohols. *J. Phys. Chem. B* **2008**, *112*, 8330–8339.

(62) Baker, S. N.; Baker, G. A.; Bright, F. V. Temperature-Dependent Microscopic Solvent Properties of 'Dry' and 'Wet' 1-Butyl-3-methylimidazolium Hexafluorophosphate: Correlation with $E_T(30)$

and Kamlet–Taft Polarity Scales. *Green Chem.* **2002**, *4*, 165–169.

(63) Lee, J.-M.; Ruckes, S.; Prausnitz, J. M. Solvent Polarities and Kamlet-Taft Parameters for Ionic Liquids Containing a Pyridinium Cation. *J. Phys. Chem. B* **2008**, *112*, 1473–1476.

(64) Khupse, N. D.; Kumar, A. Contrasting Thermosolvatochromic Trends in Pyridinium-, Pyrrolidinium-, and Phosphonium-Based Ionic Liquids. *J. Phys. Chem. B* **2010**, *114*, 376–381.

(65) Lee, J.-M.; Prausnitz, J. M. Polarity and Hydrogen-Bond-Donor Strength for Some Ionic Liquids: Effect of Alkyl Chain Length on the Pyrrolidinium Cation. *Chem. Phys. Lett.* **2010**, *492*, 55–59.

(66) Turnbull, D.; Cohen, M. H. Crystallization Kinetics and Glass Formation. In *Modern Aspects of the Vitreous State*; MacKenzie, J. D., Ed.; Butterworth, London, 1960.

(67) Yamamuro, O.; Minamimoto, Y.; Inamura, Y.; Hayashi, S.; Hamaguchi, H. Heat Capacity and Glass Transition of an Ionic Liquid 1-Butyl-3-methylimidazolium Chloride. *Chem. Phys. Lett.* **2006**, *423*, 371–375.

(68) Speck, J. M.; Korb, M.; Hildebrandt, A.; Lang, H. The Role of the Anion in the Charge Transfer Properties of Mixed-Valent Biferrocene. *Inorg. Chim. Acta* **2018**, *483*, 39–43.

(69) Kimura, Y.; Hamamoto, T.; Terazima, M. Raman Spectroscopic Study on the Solvation of *N*,*N*-Dimethyl-*p*-nitroaniline in Room-Temperature Ionic Liquids. *J. Phys. Chem. A* **2007***, 111*, 7081–7080.

(70) Vij, A.; Zheng, Y. Y.; Kirchmeier, R. L.; Shreeve, J. M. Electrophilic Addition and Substitution-Reactions of bis(Trifluoromethyl)Sulfonyl)Amide and Its N-Chloro Derivative. *Inorg. Chem*. **1994**, *33*, 3281–3288 (1994).

For Tables of Contents Use Only

Thermal Properties and Solvent Polarities of Mixed-Valence Ionic Liquids Containing Cationic Biferrocenylene Derivatives

Shota Hamada, Tomoyuki Mochida*

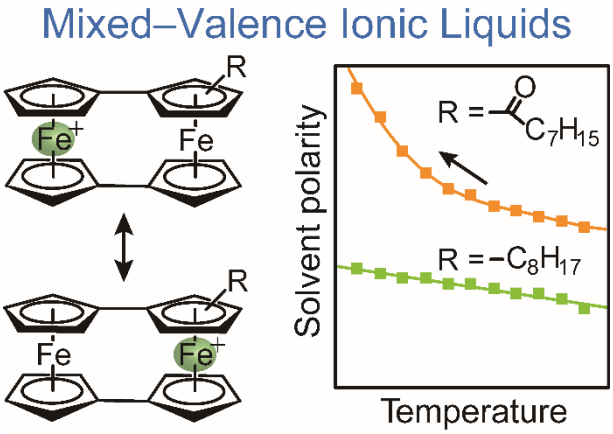

Organometallic ILs containing mixed-valence biferrocenylenium cations were synthesized. The solvent polarities of the ILs bearing acyl substituents increased significantly with decreasing temperature.

Supporting Information

Thermal Properties and Solvent Polarities of Mixed-Valence Ionic Liquids with Cationic Biferrocenylene Derivatives

Shota Hamada[†] and Tomoyuki Mochida*[†‡]

[†]*Department of Chemistry, Graduate School of Science, Kobe University, 1-1 Rokkodai, Nada, Kobe, Hyogo 657-8501, Japan. E-mail: tmochida@platinum.kobe-u.ac.jp*

[‡]*Research Center for Membrane and Film Technology, Kobe University, 1-1 Rokkodai, Nada, Kobe, Hyogo 657-8501, Japan*

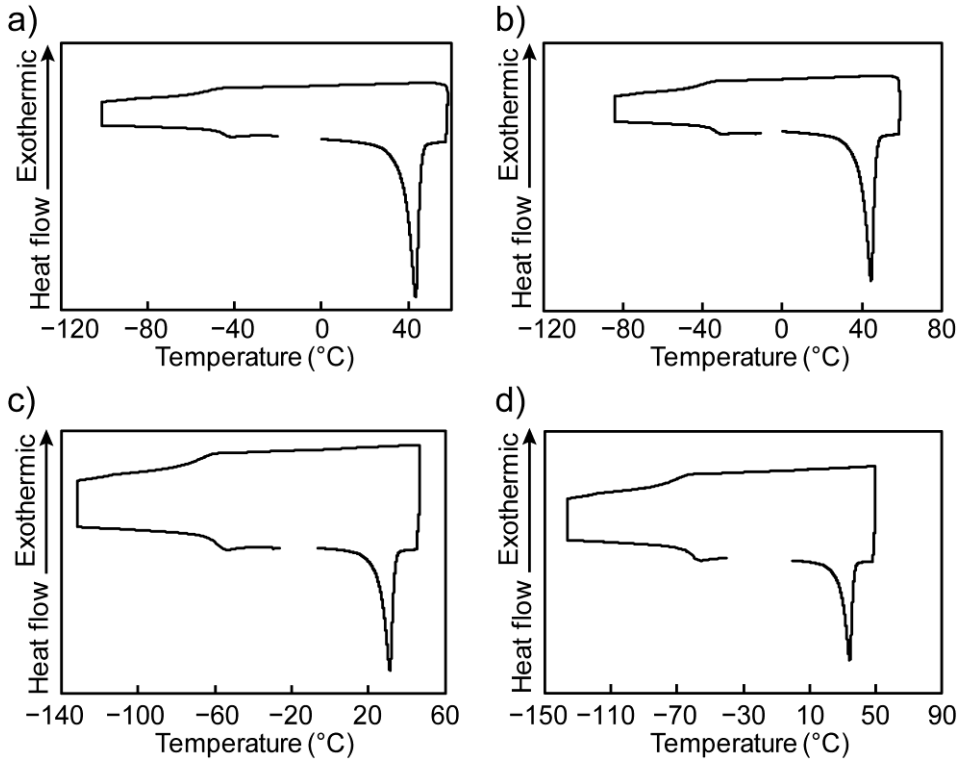

Figure S1. DSC traces of the mono-substituted BFD salts with Tf_2N: (a) **1a**, (b) **1b**, (c) **2a**, and (d) **2b**.

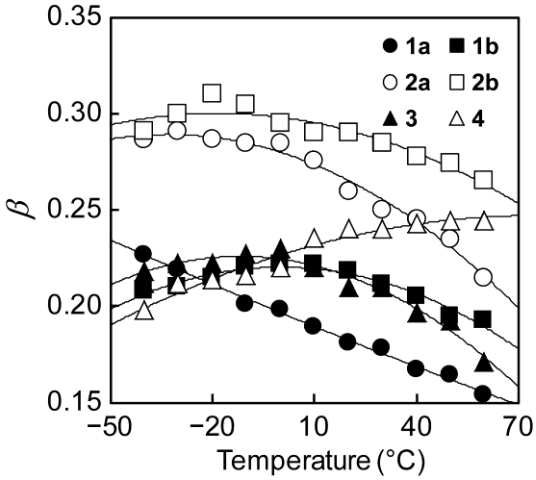

Figure S2. Temperature dependence of β for **1a, 1b, 2a, 2b, 3,** and **4**.

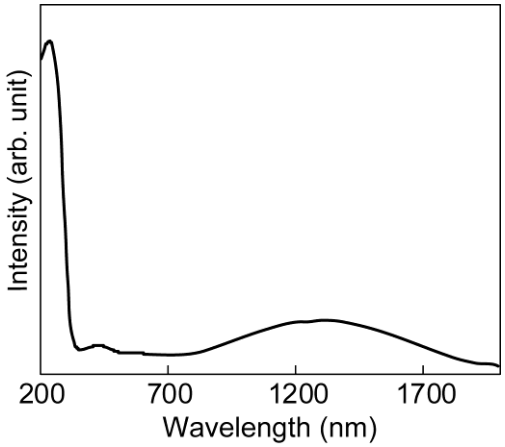

Figure S3. UV-vis-NIR spectrum of **1b** in the liquid state (20 °C).

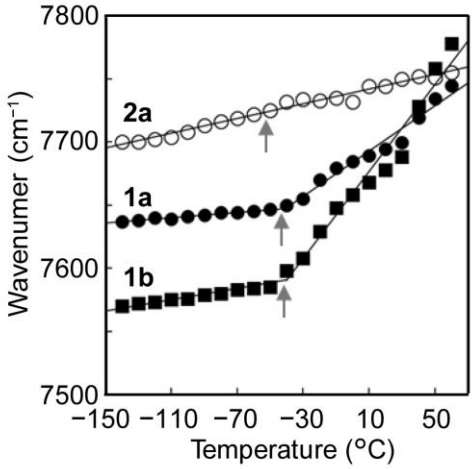

Figure S4. Temperature dependences of the IVCR energies of **1a, 1b, and 2a**. The arrows indicate the glass transition temperatures.